AIMS Mathematics, 11(3): 7847–7870.
DOI: 10.3934/math.2026324
Received: 17 January 2026
Revised: 06 March 2026
Accepted: 17 March 2026
Published: 25 March 2026

http://www.aimspress.com/journal/Math

Research article

Unified curvature modeling of surface constrained helices and associated ruled surfaces

Emad Solouma[1,*], **Ghaliah Alhamzi**[1], **Mona Bin-Asfour**[1] **and Sayed Saber**[2]

[1] Department of Mathematics and Statistics, College of Science, Imam Mohammad Ibn Saud Islamic University, Riyadh 11623, Saudi Arabia

[2] Department of Mathematics, Faculty of Science, Al-Baha University, Al-Baha 65779, Saudi Arabia

* **Correspondence:** Email: emmahmoud@imamu.edu.sa, emadms74@gmail.com.

Abstract: This paper introduces a new class of surface constrained curves, termed generalized B-helices, in the Euclidean three-space E^3. The analysis is developed through a rotational modification of the classical Darboux frame, called the $\mathbb{B}$-Darboux frame $\{T, \chi_1, \chi_2\}$. This frame combines the effects of geodesic and normal curvatures into two coupled invariants, referred to as the $\mathbb{B}$-Darboux curvatures, providing a unified description of curve geometry on regular surfaces. Within this framework, three types of generalized $\mathbb{B}$-helices are defined, and their characterization conditions are expressed in terms of these curvature functions. The spherical representations corresponding to the $\mathbb{B}$-Darboux frame vectors are also examined, and explicit relations for their curvature and torsion are derived. It is shown that each type of generalized $\mathbb{B}$-helix generates a circular indicatrix on the unit sphere, establishing a direct geometric link between spatial and spherical curves. To validate the theoretical developments, illustrative examples and graphical simulations of ruled surfaces associated with the frame vectors are presented, confirming the applicability and effectiveness of the proposed model.

Keywords: $\mathbb{B}$-Darboux frame; generalized $\mathbb{B}$-helices; surface curves; Euclidean geometry; curvature invariants
Mathematics Subject Classification: 51M04, 53A04

1. Overview and geometric motivation

The notion of helical curves has played a fundamental role in classical differential geometry since the early nineteenth century. In the Euclidean space E^3, a general helix is defined as a space curve whose tangent vector, referred to as the helix axis, maintains a constant angle with a fixed direction. The foundations of this concept were established by M. A. Lancret (1806) [22] and later rigorously formulated by Cayley (1845) [8], who proved that a space curve is helical if and only if the ratio of

its curvature to torsion remains constant. This result, known as Lancret's theorem, remains a classical reference in the study of curve geometry [8, 22].

The theory of helices has since been widely broadened through various generalizations in different geometric frameworks and using multiple types of moving frames. The Frenet–Serret frame, dependent on curvature and torsion, offers the standard local description of a space curve. However, it becomes undefined when either of these invariants vanishes, motivating the development of alternative frames that remain well-defined in such degenerate cases or when the curve is constrained to a surface.

A notable example is the Bishop frame (parallel transport frame), which eliminates torsion and yields a smoothly varying orthonormal basis even when torsion vanishes. This frame has been adapted to several geometric contexts and successfully applied to the study of slant helices and their spherical indicatrices [19–21,23–25]. In particular, Izumiya and Takeuchi (2004) [19] characterized slant helices as curves whose principal normal vector forms a constant angle with a fixed direction, extending helical behavior beyond the tangent direction. Subsequent works extended these ideas to Lorentzian [5, 18], Riemannian [4, 9], and Lie group settings [27], significantly enriching the modern theory of helices.

Another major advancement arose from the introduction of the Darboux frame $\{T, g, n\}$, which is adapted to a curve lying on a smooth surface. This frame decomposes the curvature into geodesic curvature, normal curvature, and geodesic torsion, enabling a refined analysis of surface-constrained curves and proving useful in geometry, computer-aided modeling, fiber optics, and motion mechanics.

Alternative frame constructions have also provided important insights into the geometric behavior of surface-related curves. In particular, the modified orthogonal frame (MOF) has proven effective in studying the curvature properties and invariants of ruled surfaces. Recent research extended the applicability of the MOF to Minkowski three-space, revealing strong connections with Bishop- and Darboux-type frames and motivating the development of extended frame-based formulations [6, 7, 16, 17, 31].

More recent developments include the introduction of flow-curvature concepts by Crasmareanu (2022–2023), which led to the formulation of the flow frame, a dynamically rotating version of the Frenet frame evolving along the tangent direction [10–13]. Building on these concepts, Anar et al., (2025) studied generalized helices within the flow-frame in E^3 and investigated the geometric properties of their spherical indicatrices [29], providing an alternative interpretation of Lancret's condition under rotational evolution.

Recent years have also seen growing interest in the modeling and analysis of complex dynamical processes on networks and continuous media, including spatiotemporal pattern formation, propagation phenomena, and control strategies arising in biological and information systems [26, 33]. These studies highlight the importance of geometric and structural features in the qualitative behavior of dynamical systems. While the present work does not address such modeling problems directly, it shares a common geometric viewpoint by emphasizing the role of invariant structures and curvature-based descriptions. In this sense, the $\mathbb{B}$-Darboux framework developed here may be viewed as complementary from a differential geometric perspective, providing tools that could be useful in future investigations of surface-constrained dynamics.

The present work introduces the $\mathbb{B}$-Darboux frame $\{\mathrm{T}, \chi_1, \chi_2\}$, constructed via a smooth rotation of the classical Darboux trihedron by an angle that depends on the torsion of the surface curve. This rotation couples the geodesic and normal curvature components into two curvature functions, termed the $\mathbb{B}$-Darboux curvatures. Within this unified formulation, three classes of generalized $\mathbb{B}$-helices

are defined and characterized in terms of these curvature quantities. Additionally, by transferring the $\mathbb{B}$-Darboux frame vectors to the origin of the unit sphere in E^3, we derive the corresponding spherical indicatrices and analyze their geometric relationship with the spatial helices. This formulation naturally extends concepts arising from flow-based frames to intrinsic surface geometry.

Beyond theoretical contributions, the proposed structure is relevant to practical applications in several scientific and engineering domains. In geometric modeling and computer-aided design, the $\mathbb{B}$-Darboux frame facilitates precise motion and deformation control of surface-adapted objects. In robotics and kinematics, it serves to describe the movement of mechanical systems constrained to curved environments. Moreover, in mechanics and materials science, it assists in the analysis of curvature-induced behavior in filamentary or surface-bound configurations, consistent with recent advances in flow-frame geometry [13], helix theory [29], and ruled surface models employing modified orthogonal frames in Minkowski space [31].

Several moving frame constructions have been introduced in the literature to study the geometry of space curves and surface constrained curves, including the Frenet-Serret frame, the Bishop (parallel transport) frame, and the classical Darboux frame. Each of these frameworks possesses specific advantages and limitations depending on the geometric setting.

The Frenet frame provides a complete local description of a space curve through its curvature and torsion; however, it becomes undefined when the curvature vanishes. The Bishop frame resolves this degeneracy by eliminating torsion, but it is not adapted to curves constrained to surfaces and does not explicitly capture intrinsic and extrinsic curvature effects. The Darboux frame is naturally adapted to surface curves and separates curvature into geodesic and normal components, yet its formulation does not unify these quantities into a single invariant description.

The $\mathbb{B}$-Darboux frame proposed in this work is obtained by a torsion dependent rotation of the classical Darboux frame about the tangent direction. This construction yields two coupled curvature invariants (ζ_1, ζ_2) that encode both intrinsic and extrinsic curvature effects in a unified manner, while preserving orthonormality and regularity along the curve.

A concise comparison of the principal features of the Frenet, Bishop, Darboux, and $\mathbb{B}$-Darboux frames is presented in Table 1.

Table 1. Comparison of moving frame formulations for curves in $\mathbb{E}^3$.

Frame	Torsion-dependent	Surface-adapted	Degeneracy-free	Unified curvature
Frenet-Serret	Yes	No	No	No
Bishop	No	No	Yes	No
Darboux	Yes	Yes	Partial	No
$\mathbb{B}$-Darboux	Yes (nonlocal)	Yes	Yes	Yes

Existing formulations of curve theory in Euclidean three-space are primarily developed for free curves and therefore face difficulties when applied to curves constrained to lie on surfaces. In particular, the Frenet frame depends on the regular behavior of torsion and may lose stability at points where the torsion vanishes or changes sign. Alternative constructions such as the Bishop frame ensure continuity but remain purely curve based and do not reflect the interaction between the curve and the geometry of the supporting surface. Although the Darboux frame incorporates surface normals and tangential directions, it does not resolve torsion-related degeneracies, nor does it provide a systematic mechanism

for linking constant-angle conditions with global geometric features such as spherical indicatrices. These observations indicate the need for a surface-adapted and torsion regular description of surface constrained curves, which motivates the framework developed in this work.

The remainder of the paper is organized as follows. Section 2 presents the preliminaries and formulates the $\mathbb{B}$-Darboux frame along a surface curve, including the underlying curvature relations and transformation properties. In Section 3, three types of generalized $\mathbb{B}$-helices (Type-I, Type-II, and Type-III) are introduced, and their characterization results are established. Section 4 is devoted to the analysis of the spherical images of the vectors T, χ_1, and χ_2, including curvature and torsion formulae and their connection to the spatial helices. Section 5 illustrates the theoretical results through detailed examples and graphical visualizations, including both developable and non-developable ruled surfaces generated by χ_1 and χ_2. Finally, the paper concludes with a summary of the main contributions and possible directions for future research.

2. Foundations of curve geometry on surfaces

Let E^3 denote the three-dimensional Euclidean space endowed with the standard inner product

$$\langle a, b\rangle = a_1b_1 + a_2b_2 + a_3b_3,$$

for any two vectors $a = (a_1, a_2, a_3)$ and $b = (b_1, b_2, b_3) \in \mathrm{E}^3$. The corresponding Euclidean norm is given by $\|a\| = \sqrt{\langle a, a\rangle}$. The cross product of a and b can be represented as

$$a \times b = \det\begin{pmatrix} e_1 & e_2 & e_3 \\ a_1 & a_2 & a_3 \\ b_1 & b_2 & b_3 \end{pmatrix},$$

where $\{e_1, e_2, e_3\}$ denotes the canonical orthonormal basis of E^3.

A differentiable curve $\varphi : I \subset \mathbb{R} \to \mathrm{E}^3$ is said to be regular if $\varphi'(s) \neq 0$ for all $s \in I$. When $\|\varphi'(s)\| = 1$, the curve is said to be parameterized by arc length and called a unit-speed curve.

Let $\{\mathrm{T}, \mathrm{N}, \mathrm{B}\}$ denote the Frenet frame of the regular curve $\varphi = \varphi(\sigma)$ in E^3, associated with the curvature ζ and torsion τ. The Frenet equations are expressed as [15, 32]:

$$\begin{bmatrix} \mathrm{T}(\sigma) \\ \mathrm{N}(\sigma) \\ \mathrm{B}(\sigma) \end{bmatrix}_{\sigma} = \begin{bmatrix} 0 & \zeta(\sigma) & 0 \\ -\zeta(\sigma) & 0 & \tau(\sigma) \\ 0 & -\tau(\sigma) & 0 \end{bmatrix} \begin{bmatrix} \mathrm{T}(\sigma) \\ \mathrm{N}(\sigma) \\ \mathrm{B}(\sigma) \end{bmatrix}, \tag{2.1}$$

such that $\langle \mathrm{T}, \mathrm{N}\rangle = \langle \mathrm{T}, \mathrm{B}\rangle = \langle \mathrm{N}, \mathrm{B}\rangle = 0$ and $\langle \mathrm{T}, \mathrm{T}\rangle = \langle \mathrm{N}, \mathrm{N}\rangle = \langle \mathrm{B}, \mathrm{B}\rangle = 1$.

Suppose that $\mathbb{M}$ is an oriented smooth surface that has been provided by a position vector field $\Psi(u, v)$ and submerged in E^3. Assume that the unit-speed curve $\varphi(\sigma) = \Psi(u(\sigma), v(\sigma))$ lies on $\mathbb{M}$. Denote the unit normal to the surface $\mathbb{M}$ along φ by n and the unit tangent vector to φ by T. The vector $g = n \times \mathrm{T}$ is perpendicular to T and is located on the tangent plane of $\mathbb{M}$. The Darboux frame of the curve is thus an orthonormal moving frame along φ formed by the arranged set $\{\mathrm{T}, g, n\}$.

The geodesic curvature ζ_g, the normal curvature ζ_n, and the geodesic torsion τ_g of φ on $\mathbb{M}$ influence the derivatives of the Darboux frame vectors. The curvature of $\mathbb{M}$ in the normal direction, the rotating

of the surface normal along the curve, and the bending of φ within the tangent plane are all described by these values, respectively. The traditional Darboux equations are satisfied by them [15, 32]:

$$\begin{bmatrix} \mathrm{T}(\sigma) \\ g(\sigma) \\ n(\sigma) \end{bmatrix}_{\sigma} = \begin{bmatrix} 0 & \zeta_g(\sigma) & \zeta_n(\sigma) \\ -\zeta_g(\sigma) & 0 & \tau_g(\sigma) \\ -\zeta_n(\sigma) & -\tau_g(\sigma) & 0 \end{bmatrix} \begin{bmatrix} \mathrm{T}(\sigma) \\ g(\sigma) \\ n(\sigma) \end{bmatrix}, \tag{2.2}$$

where

$$\zeta_g = \langle \mathrm{T}', g \rangle, \qquad \zeta_n = \langle \mathrm{T}', n \rangle, \qquad \tau_g = \langle g', n \rangle.$$

Consider the unit-speed curve $\varphi(\sigma)$ on the surface $\mathbb{M} = \Psi(u, v)$. For φ, the $\mathbb{B}$-Darboux frame $\{\mathrm{T}, \chi_1, \chi_2\}$ evolves as follows [2, 3, 14, 30]:

$$\begin{bmatrix} \mathrm{T}(\sigma) \\ \chi_1(\sigma) \\ \chi_2(\sigma) \end{bmatrix}_{\sigma} = \begin{bmatrix} 0 & \zeta_1(\sigma) & \zeta_2(\sigma) \\ -\zeta_1(\sigma) & 0 & 0 \\ -\zeta_2(\sigma) & 0 & 0 \end{bmatrix} \begin{bmatrix} \mathrm{T}(\sigma) \\ \chi_1(\sigma) \\ \chi_2(\sigma) \end{bmatrix}, \tag{2.3}$$

where ζ_1 and ζ_2 are called the $\mathbb{B}$-Darboux curvatures, defined as

$$\begin{aligned} \zeta_1 &= \zeta_g \sin\vartheta + \zeta_n \cos\vartheta, \\ \zeta_2 &= \zeta_n \sin\vartheta - \zeta_g \cos\vartheta, \\ \zeta_g^2 + \zeta_n^2 &= \zeta_1^2 + \zeta_2^2. \end{aligned} \tag{2.4}$$

The transformation matrix in Eq (2.4) describes a local rotation of the Darboux frame $\{\mathrm{T}, g, n\}$ around the tangent direction T by the angle $\vartheta(\sigma)$. This rotation generates the $\mathbb{B}$-Darboux frame $\{\mathrm{T}, \chi_1, \chi_2\}$ while preserving orthogonality and unit length of the frame vectors. Geometrically, the transformation couples the geodesic and normal curvature effects into the new curvature components (ζ_1, ζ_2), allowing the curve's intrinsic and extrinsic properties on the surface to be represented in a single, coherent framework. The two frames $\{\mathrm{T}, g, n\}$ and $\{\mathrm{T}, \chi_1, \chi_2\}$ are related through the transformation

$$\begin{bmatrix} \mathrm{T}(\sigma) \\ \chi_1(\sigma) \\ \chi_2(\sigma) \end{bmatrix} = \begin{bmatrix} 1 & 0 & 0 \\ 0 & \sin\vartheta & \cos\vartheta \\ 0 & -\cos\vartheta & \sin\vartheta \end{bmatrix} \begin{bmatrix} \mathrm{T}(\sigma) \\ g(\sigma) \\ n(\sigma) \end{bmatrix}, \tag{2.5}$$

where the angle ϑ between n and χ_1 satisfies

$$\vartheta(\sigma) = \int_0^{\sigma} \tau(\sigma)\, d\sigma + \vartheta_0, \qquad \vartheta_0 = \vartheta(0).$$

Remark 2.1. *The rotation angle $\vartheta(\sigma)$ depends on the integral of the torsion $\tau(\sigma)$, which introduces a nonlocal relationship between them. In this work, we restrict our attention to smooth regular curves for which $\tau(\sigma)$ is a continuous and differentiable function. Under this assumption, $\vartheta(\sigma)$ is well defined, and the $\mathbb{B}$-Darboux frame $\{\mathrm{T}, \chi_1, \chi_2\}$ remains an orthonormal and continuous moving frame along the curve. If the torsion becomes discontinuous or undefined, a piecewise or generalized formulation of $\vartheta(\sigma)$ would be necessary, which may be considered in future investigations.*

Since the transformation matrix given in Eq (2.5) is orthogonal, the triad $\{T, \chi_1, \chi_2\}$ constitutes an orthonormal system along the surface curve, satisfying $\langle T, \chi_1\rangle = \langle T, \chi_2\rangle = \langle \chi_1, \chi_2\rangle = 0$ and $\langle \chi_1, \chi_1\rangle = \langle \chi_2, \chi_2\rangle = 1$. This statement clarifies that the orthonormality of the $\mathbb{B}$-Darboux frame is preserved and fully consistent with that of the classical Darboux frame.

3. Helical surface curves under a rotated Darboux-type frame

The $\mathbb{B}$-Darboux frame $\{T, \chi_1, \chi_2\}$ of a regular unit-speed curve $\varphi(\sigma)$ resting on a smooth oriented surface $\mathbb{M} \subset E^3$ is represented by the three different classes of generalized $\mathbb{B}$-helices that we describe and examine in this section. A rotational version of the conventional Darboux frame, the $\mathbb{B}$-Darboux frame represents the curve through its curvature components ζ_1 and ζ_2, which fulfill the equation $\zeta = \sqrt{\zeta_1^2 + \zeta_2^2}$. It is assumed that all of the values mentioned below are specified with respect to the arc-length parameter σ and are smooth.

Keeping a consistent angle between one of the vectors of a moving frame and a fixed direction in the ambient space is what defines the idea of a $\mathbb{B}$-helix. Three possibilities emerge based on which frame vector keeps this angular constancy with a fixed unit vector $\mathbf{d} \in E^3$.

Definition 3.1. Suppose that the vectors T, χ_1, and χ_2, respectively, maintain a constant angle with $\mathbf{d}$ on a regular surface $\mathbb{M}$ equipped with the $\mathbb{B}$-Darboux frame $\{T, \chi_1, \chi_2\}$. The $\varphi(\sigma)$ unit-speed curve is referred to as the Type-I, Type-II, and Type-II generalized $\mathbb{B}$-helix, respectively. $\mathbf{d}$ is referred to as the axis of the helix in each of the three scenarios.

A surface curve of the first kind has a tangent direction that maintains a constant inclination with respect to a spatial axis. The well-known concept of the Lancret helix is extended to the $\mathbb{B}$-Darboux framework in this description.

Remark 3.1. *The notion of generalized $\mathbb{B}$-helices introduced in this work differs fundamentally from classical helix characterizations based on Frenet, Bishop, or Darboux frames. In the Frenet and Bishop settings, helix conditions are expressed solely in terms of curve-based invariants, while the classical Darboux formulation incorporates surface geometry but does not involve torsion-dependent frame rotations. In contrast, the $\mathbb{B}$-Darboux helices are defined through constant-angle conditions involving surface-adapted, torsion regular directions, leading to curvature invariants (ζ_1, ζ_2) with a distinct geometric interpretation. Moreover, the resulting helix types are not, in general, equivalent to one another under rigid motions or reparameterizations, as they impose different invariant constraints on the $\mathbb{B}$-Darboux curvatures and their associated spherical indicatrices.*

Theorem 3.1. *Consider a unit-speed curve $\varphi(\sigma)$ on a surface $\mathbb{M}$ that has the $\mathbb{B}$-Darboux frame $\{T, \chi_1, \chi_2\}$. Then φ is a Type-I generalized $\mathbb{B}$-helix if and only if*

$$\frac{\zeta_1}{\zeta_2} = \textit{constant}. \tag{3.1}$$

Proof. Assume that $\phi(\sigma)$ is a Type-I generalized $\mathbb{B}$-helix. By definition, the tangent vector T makes a constant angle α with a fixed unit vector $\mathbf{d} \in \mathbb{E}^3$, that is,

$$\langle T, \mathbf{d}\rangle = \cos\alpha = \text{constant}.$$

Differentiating with respect to the arc length parameter σ yields

$$\langle \mathrm{T}', d\rangle = 0.$$

Using the $\mathbb{B}$-Darboux frame relation

$$\mathrm{T}' = \zeta_1\chi_1 + \zeta_2\chi_2,$$

we obtain

$$\zeta_1\langle \chi_1, \mathbf{d}\rangle + \zeta_2\langle \chi_2, \mathbf{d}\rangle = 0.$$

Dividing by $\langle \chi_2, \mathbf{d}\rangle \neq 0$ gives

$$\frac{\langle \chi_1, \mathbf{d}\rangle}{\langle \chi_2, \mathbf{d}\rangle} = -\frac{\zeta_2}{\zeta_1}.$$

Since the fixed vector $\mathbf{d}$ and the $\mathbb{B}$-Darboux frame vectors χ_1 and χ_2 depend smoothly on σ, the functions $\langle \chi_1, d\rangle$ and $\langle \chi_2, \mathbf{d}\rangle$ are smooth along the curve. Hence, whenever $\langle \chi_2, \mathbf{d}\rangle \neq 0$, the ratio $\frac{\langle \chi_1, \mathbf{d}\rangle}{\langle \chi_2, d\rangle}$ is constant. Consequently, the above relation implies that $\frac{\zeta_1}{\zeta_2}$ = constant. Conversely, if ζ_1/ζ_2 is constant, then there exists a fixed unit vector $\mathbf{d}$ such that $\langle \mathrm{T}, \mathbf{d}\rangle$ remains constant along the curve, and hence $\phi(\sigma)$ is a Type-I generalized $\mathbb{B}$-helix. □

Remark 3.2. *If $\vartheta(\sigma) = 0$, then $\zeta_1 = \zeta_g$ and $\zeta_2 = \zeta_n$, and the above condition reduces to $\zeta_g/\zeta_n =$ constant, which is precisely the classical surface helix condition.*

Theorem 3.2. *The unit-speed curve φ is Type-I generalized $\mathbb{B}$-helix if the condition is met:*

$$\det(\mathrm{T}', \mathrm{T}'', \mathrm{T}''') = 0. \tag{3.2}$$

Proof. By differentiating the frame equations successively, one finds

$$\det(\mathrm{T}', \mathrm{T}'', \mathrm{T}''') = \mu_1'\left(\frac{1}{\mu_1^2}\right)(\zeta_1^2 + \zeta_2^2)^{5/2},$$

where

$$\mu_1(\sigma) = \frac{[(\frac{\zeta_1}{\zeta_2})\zeta_1 + \zeta_2]\sqrt{1 + (\frac{\zeta_1}{\zeta_2})^2}}{(\frac{\zeta_1}{\zeta_2})' - \zeta_1[1 + (\frac{\zeta_1}{\zeta_2})^2]}.$$

Hence, $\det(\mathrm{T}', \mathrm{T}'', \mathrm{T}''') = 0$ if and only if $\mu_1' = 0$, that is, μ_1 is constant. □

Theorem 3.3. *Consider a unit-speed curve $\varphi(\sigma)$ on a surface $\mathbb{M}$ with a $\mathbb{B}$-Darboux frame $\{\mathrm{T}, \chi_1, \chi_2\}$. Then φ is a Type-II generalized $\mathbb{B}$-helix if and only if*

$$\frac{d}{d\sigma}\left(\frac{\zeta_2}{\zeta}\right) + \tau\left(\frac{\zeta_1}{\zeta}\right) = 0, \tag{3.3}$$

where $\zeta = \sqrt{\zeta_1^2 + \zeta_2^2}$ and $\tau = d\vartheta/d\sigma$.

Proof. Assume that $\varphi(\sigma)$ is a Type-II generalized $\mathbb{B}$-helix. By definition, the vector χ_1 makes a constant angle β with a fixed unit vector $\mathbf{d} \in \mathbb{E}^3$, that is,

$$\langle \chi_1, \mathbf{d} \rangle = \cos\beta = \text{constant}. \tag{3.4}$$

Differentiating (3.4) with respect to the arc length parameter σ yields $\langle \chi_1', \mathbf{d} \rangle = 0$. Using the $\mathbb{B}$-Darboux relation $\chi_1' = -\zeta_1 \mathrm{T}$, we obtain

$$\langle \mathrm{T}, \mathbf{d} \rangle = 0. \tag{3.5}$$

Differentiating (3.5) once more with respect to σ gives $\langle \mathrm{T}', \mathbf{d} \rangle = 0$. From the $\mathbb{B}$-Darboux equation

$$T' = \zeta_1 \chi_1 + \zeta_2 \chi_2,$$

the equation becomes

$$\zeta_1 \langle \chi_1, \mathbf{d} \rangle + \zeta_2 \langle \chi_2, \mathbf{d} \rangle = 0. \tag{3.6}$$

Let ϑ denote the angle between χ_2 and $\mathbf{d}$. Then

$$\langle \chi_1, \mathbf{d} \rangle = \frac{\zeta_2}{\zeta}, \qquad \langle \chi_2, \mathbf{d} \rangle = -\frac{\zeta_1}{\zeta},$$

where $\zeta = \sqrt{\zeta_1^2 + \zeta_2^2}$. Substituting into (3.6) and differentiating with respect to σ, we obtain

$$\frac{d}{d\sigma}\left(\frac{\zeta_2}{\zeta}\right) + \tau\left(\frac{\zeta_1}{\zeta}\right) = 0,$$

which proves Eq (3.3).

Conversely, if condition (3.3) holds, then the vector

$$\mathbf{d} = \frac{\zeta_2}{\zeta}\chi_1 - \frac{\zeta_1}{\zeta}\chi_2$$

is constant along $\varphi(\sigma)$, and hence χ_1 makes a constant angle with $\mathbf{d}$. Therefore, $\varphi(\sigma)$ is a Type-II generalized $\mathbb{B}$-helix. □

Remark 3.3. *If $\tau = 0$, then $\frac{d}{d\sigma}\left(\frac{\zeta_2}{\zeta}\right) = 0$, so that ζ_2/ζ remains constant. This corresponds to the condition of a Bishop-type slant helix.*

Remark 3.4. *Within the $\mathbb{B}$-Darboux framework, the curvature components ζ_1 and ζ_2 serve as combined measures that incorporate both geodesic and normal curvature influences. This representation provides a compact way to describe the bending behavior of a curve on a surface without losing the distinction between the underlying curvature types. The classical quantities κ_g and κ_n can be directly recovered from ζ_1 and ζ_2 using*

$$\kappa_g = \zeta_1 \cos\vartheta - \zeta_2 \sin\vartheta, \qquad \kappa_n = \zeta_1 \sin\vartheta + \zeta_2 \cos\vartheta,$$

where ϑ denotes the rotation angle relating the $\mathbb{B}$-Darboux frame to the traditional Darboux system. Hence, although ζ_1 and ζ_2 combine intrinsic and extrinsic curvature effects into a unified form, their physical significance relevant to areas such as elasticity, optics, and biophysics remains clearly interpretable.

The parameters ζ_1 and ζ_2 arise from a rotational transformation of the classical geodesic and normal curvatures, κ_g and κ_n, respectively. From a geometric standpoint, these quantities reflect how the intrinsic and extrinsic curvature properties of a surface constrained curve interact within the $\mathbb{B}$-Darboux frame, offering a coherent and generalized description of local curvature behavior.

Theorem 3.4. *Let $\varphi(\sigma)$ be a unit-speed curve on a surface $\mathbb{M}$ with the $\mathbb{B}$-Darboux frame $\{\mathrm{T}, \chi_1, \chi_2\}$. The curve φ is a Type-II generalized $\mathbb{B}$-helix if and only if*

$$\det(\chi_1', \chi_1'', \chi_1''') = 0. \tag{3.7}$$

Proof. Let $\varphi(\sigma)$ be a unit-speed curve with the $\mathbb{B}$-Darboux frame $\{\mathrm{T}, \chi_1, \chi_2\}$. From the $\mathbb{B}$-Darboux equations, we have

$$\chi_1' = -\zeta_1 \mathrm{T},$$

and hence

$$\chi_1'' = -\zeta_1' \mathrm{T} - \zeta_1 \mathrm{T}'.$$

Using

$$\mathrm{T}' = \zeta_1 \chi_1 + \zeta_2 \chi_2,$$

it follows that

$$\chi_1'' = -\zeta_1' \mathrm{T} - \zeta_1(\zeta_1 \chi_1 + \zeta_2 \chi_2).$$

Differentiating once more yields

$$\chi_1''' = -\zeta_1'' \mathrm{T} - 2\zeta_1' \mathrm{T}' - \zeta_1(\zeta_1' \chi_1 + \zeta_2' \chi_2) - \zeta_1(\zeta_1 \chi_1' + \zeta_2 \chi_2').$$

Substituting $\chi_1' = -\zeta_1 \mathrm{T}$ and $\chi_2' = -\zeta_2 \mathrm{T}$ and arranging the coefficients with respect to the basis $\{\mathrm{T}, \chi_1, \chi_2\}$, a direct computation gives

$$\det(\chi_1', \chi_1'', \chi_1''') = \zeta_1^3 \zeta_2^2 \left(\frac{\zeta_1}{\zeta_2}\right)'.$$

Therefore,

$$\det(\chi_1', \chi_1'', \chi_1''') = 0 \quad \Longleftrightarrow \quad \left(\frac{\zeta_1}{\zeta_2}\right)' = 0.$$

By Theorem 3.3, this condition is equivalent to $\varphi(\sigma)$ being a Type-II generalized $\mathbb{B}$-helix. This completes the proof. □

Theorem 3.5. *Consider a unit-speed curve $\varphi(\sigma)$ on a surface $\mathbb{M}$ with the $\mathbb{B}$-Darboux frame $\{T, \chi_1, \chi_2\}$. Then φ is a Type-III generalized $\mathbb{B}$-helix if and only if*

$$\frac{d}{d\sigma}\left(\frac{\zeta_1}{\zeta}\right) - \tau\left(\frac{\zeta_2}{\zeta}\right) = 0. \tag{3.8}$$

Proof. Assume $\langle \chi_2, \mathbf{d} \rangle = \cos\gamma$ is constant. Differentiating gives $\langle \chi_2', \mathbf{d} \rangle = 0$. Since $\chi_2' = -\zeta_2 \mathrm{T}$, it follows that $\langle \mathrm{T}, \mathbf{d} \rangle = 0$. Differentiating once again and applying (2.3) yields

$$\frac{d}{d\sigma}\left(\frac{\zeta_1}{\zeta}\right) - \tau\left(\frac{\zeta_2}{\zeta}\right) = 0,$$

which completes the proof. □

Remark 3.5. *If $\tau = 0$, then ζ_1/ζ is constant, corresponding to the Bishop-type helix. Hence, the generalized $\mathbb{B}$-helices encompass the Frenet, Darboux, and Bishop helical structures as special cases.*

Theorem 3.6. *Let $\varphi(\sigma)$ be a unit-speed curve on a surface $\mathbb{M}$ with the $\mathbb{B}$-Darboux frame $\{T, \chi_1, \chi_2\}$. The curve φ is a Type-III generalized $\mathbb{B}$-helix if and only if*

$$\det(\chi_2', \chi_2'', \chi_2''') = 0. \tag{3.9}$$

Proof. Direct calculation gives

$$\det(\chi_2', \chi_2'', \chi_2''') = \mu_3' \left(\frac{1}{\mu_3^2}\right)(\zeta_1^2 + \zeta_2^2)^{5/2},$$

where

$$\mu_3(\sigma) = \frac{[(\frac{\zeta_2}{\zeta_1})\zeta_2 + \zeta_1]\sqrt{1 + (\frac{\zeta_2}{\zeta_1})^2}}{(\frac{\zeta_2}{\zeta_1})' - \zeta_2[1 + (\frac{\zeta_2}{\zeta_1})^2]}.$$

Thus, $\det(\chi_2', \chi_2'', \chi_2''') = 0$ if and only if $\mu_3' = 0$. □

Proposition 3.1. *Let $\varphi(\sigma)$ be a unit-speed curve on a surface $\mathbb{M}$ endowed with the $\mathbb{B}$-Darboux frame $\{\mathrm{T}, \chi_1, \chi_2\}$. Then each $\mathbb{B}$-helix type defined by a constant-angle condition between T and a fixed direction is equivalent to the circularity of a specific spherical indicatrix associated with χ_1 or χ_2.*

Remark 3.6. *This equivalence is not available within the classical Darboux framework. Indeed, the classical Darboux theory involves only the frame $\{\mathrm{T}, g, n\}$ and its associated invariants $(\kappa_g, \kappa_n, \tau_g)$, and does not introduce torsion-dependent rotations of surface-adapted directions. As a consequence, the spherical indicatrices of the $\mathbb{B}$-Darboux vectors χ_1 and χ_2 and their circularity properties do not arise in the classical Darboux literature.*

Theorem 3.7. *The three $\mathbb{B}$-helix types defined by constant-angle conditions with respect to the $\mathbb{B}$-Darboux frame are, in general, not equivalent to one another under reparameterization or rigid motions of $\mathbb{E}^3$.*

Proof. Each $\mathbb{B}$-helix type is characterized by a distinct constant-angle condition involving different $\mathbb{B}$-Darboux directions and therefore imposes different functional constraints on the $\mathbb{B}$-Darboux curvatures (ζ_1, ζ_2). Since rigid motions preserve angles and reparameterizations do not alter these invariant relations, such transformations cannot convert one $\mathbb{B}$-helix type into another unless additional restrictive conditions are imposed. Hence, the three helix types are generically inequivalent. □

4. Spherical representations induced by the rotated frame

Consider a unit-speed curve $\varphi(\sigma)$ lying on a smooth surface $\mathbb{M} \subset \mathrm{E}^3$, where the motion of the curve is described by the $\mathbb{B}$-Darboux frame $\{\mathrm{T}, \chi_1, \chi_2\}$. When the frame vectors are positioned with their tails at the origin of the unit sphere $\mathbb{S}^2 \subset \mathrm{E}^3$, they trace out three distinct spherical indicatrices:

$$\psi_{\mathrm{T}}(\sigma_{\mathrm{T}}) = \mathrm{T}(\sigma), \qquad \psi_{\chi_1}(\sigma_{\chi_1}) = \chi_1(\sigma), \qquad \psi_{\chi_2}(\sigma_{\chi_2}) = \chi_2(\sigma),$$

which are respectively referred to as the tangent, χ_1-, and χ_2-spherical images of φ. Each of these images lies on $\mathbb{S}^2$ and possesses its own curvature and torsion, which are determined in the following subsections.

4.1. Tangent spherical image ψ_{T}

The tangent spherical image of φ is defined by

$$\psi_{\mathrm{T}}(\sigma_{\mathrm{T}}) = \mathrm{T}(\sigma), \qquad \mathrm{T}(\sigma) \in \mathbb{S}^2. \tag{4.1}$$

Differentiating with respect to σ and using the $\mathbb{B}$-Darboux frame relations yields

$$\mathrm{T}' = \zeta_1\chi_1 + \zeta_2\chi_2.$$

Thus,

$$\frac{d\sigma_{\mathrm{T}}}{d\sigma} = \|\mathrm{T}'\| = \zeta = \sqrt{\zeta_1^2 + \zeta_2^2},$$

so that ψ_{T} is a unit-speed curve on $\mathbb{S}^2$ when parametrized by σ_{T}.

Theorem 4.1. *The curvature ζ_{T} and torsion τ_{T} of the tangent spherical image ψ_{T} are given by*

$$\zeta_{\mathrm{T}} = \frac{\sqrt{(\zeta_1' - \zeta_2\tau)^2 + (\zeta_2' + \zeta_1\tau)^2}}{\zeta^2}, \tag{4.2}$$

$$\tau_{\mathrm{T}} = \frac{\zeta_1\zeta_2'' - \zeta_2\zeta_1'' + (\zeta_1^2 + \zeta_2^2)\tau' + 2(\zeta_1'\zeta_2 - \zeta_2'\zeta_1)\tau}{(\zeta_1' - \zeta_2\tau)^2 + (\zeta_2' + \zeta_1\tau)^2}. \tag{4.3}$$

Proof. Differentiating $\mathrm{T}' = \zeta_1\chi_1 + \zeta_2\chi_2$ gives

$$\mathrm{T}'' = (\zeta_1' - \zeta_2\tau)\chi_1 + (\zeta_2' + \zeta_1\tau)\chi_2 - (\zeta_1^2 + \zeta_2^2)\mathrm{T}.$$

Further differentiation yields

$$\begin{aligned}\mathrm{T}''' = {} & (\zeta_1'' - 2\zeta_2'\tau - \zeta_2\tau' - \zeta_1\tau^2 - \zeta_1\zeta^2)\chi_1 \\ & + (\zeta_2'' + 2\zeta_1'\tau + \zeta_1\tau' - \zeta_2\tau^2 - \zeta_2\zeta^2)\chi_2 - (2\zeta_1\zeta_1' + 2\zeta_2\zeta_2')\mathrm{T}.\end{aligned}$$

Using $\zeta_{\mathrm{T}} = \|\mathrm{T}' \times \mathrm{T}''\|/\|\mathrm{T}'\|^3$ gives (4.2), and substituting into $\tau_{\mathrm{T}} = (\mathrm{T}', \mathrm{T}'', \mathrm{T}''')/\|\mathrm{T}' \times \mathrm{T}''\|^2$ yields (4.3). □

Remark 4.1. *When $\tau = 0$, one has $\zeta_1 = \zeta_g$ and $\zeta_2 = \zeta_n$, and Eqs* (4.2) *and* (4.3) *reduce to the well known Darboux tangent indicatrix formulas.*

4.2. χ_1-spherical image ψ_{χ_1}

The χ_1-spherical image of φ is defined as

$$\psi_{\chi_1}(\sigma_{\chi_1}) = \chi_1(\sigma), \qquad \chi_1(\sigma) \in \mathbb{S}^2. \tag{4.4}$$

Differentiation gives $\chi_1' = -\zeta_1\mathrm{T}$, and thus

$$\frac{d\sigma_{\chi_1}}{d\sigma} = \|\chi_1'\| = |\zeta_1|.$$

Theorem 4.2. *The curvature ζ_{χ_1} and torsion τ_{χ_1} of ψ_{χ_1} are expressed by*

$$\zeta_{\chi_1} = \frac{\sqrt{\zeta^2 + \left(\frac{\zeta_1'}{\zeta_1}\right)^2}}{|\zeta_1|}, \tag{4.5}$$

$$\tau_{\chi_1} = \frac{\zeta_1^2\tau + \zeta_1\zeta_2' - \zeta_2\zeta_1'}{\zeta^2 + \left(\frac{\zeta_1'}{\zeta_1}\right)^2}. \tag{4.6}$$

Proof. From $\chi_1' = -\zeta_1 \mathrm{T}$, differentiating twice gives

$$\chi_1'' = -\zeta_1'\mathrm{T} - \zeta_1(\zeta_1\chi_1 + \zeta_2\chi_2),$$
$$\chi_1''' = -\zeta_1''\mathrm{T} - 2\zeta_1'(\zeta_1\chi_1 + \zeta_2\chi_2) - \zeta_1[(\zeta_1' - \zeta_2\tau)\chi_1 + (\zeta_2' + \zeta_1\tau)\chi_2 - \zeta^2\mathrm{T}].$$

Using the relations

$$\zeta_{\chi_1} = \frac{\|\chi_1' \times \chi_1''\|}{\|\chi_1'\|^3}, \qquad \tau_{\chi_1} = \frac{(\chi_1', \chi_1'', \chi_1''')}{\|\chi_1' \times \chi_1''\|^2},$$

gives (4.5) and (4.6). □

Remark 4.2. *When $\tau = 0$, these expressions reduce to the corresponding relations for the first Bishop spherical indicatrix.*

4.3. χ_2-spherical image ψ_{χ_2}

The χ_2-spherical image is defined by

$$\psi_{\chi_2}(\sigma_{\chi_2}) = \chi_2(\sigma), \qquad \chi_2(\sigma) \in \mathbb{S}^2. \tag{4.7}$$

Differentiation gives $\chi_2' = -\zeta_2 \mathrm{T}$, and hence

$$\frac{d\sigma_{\chi_2}}{d\sigma} = |\zeta_2|.$$

Theorem 4.3. *The curvature ζ_{χ_2} and torsion τ_{χ_2} of ψ_{χ_2} are*

$$\zeta_{\chi_2} = \frac{\sqrt{\zeta^2 + \left(\frac{\zeta_2'}{\zeta_2}\right)^2}}{|\zeta_2|}, \tag{4.8}$$

$$\tau_{\chi_2} = \frac{\zeta_2^2\tau - \zeta_1\zeta_2' + \zeta_2\zeta_1'}{\zeta^2 + \left(\frac{\zeta_2'}{\zeta_2}\right)^2}. \tag{4.9}$$

Proof. Differentiating $\chi_2' = -\zeta_2 \mathrm{T}$ twice and applying the frame relations gives

$$\chi_2'' = -\zeta_2'\mathrm{T} - \zeta_2(\zeta_1\chi_1 + \zeta_2\chi_2),$$
$$\chi_2''' = -\zeta_2''\mathrm{T} - 2\zeta_2'(\zeta_1\chi_1 + \zeta_2\chi_2) - \zeta_2[(\zeta_1' - \zeta_2\tau)\chi_1 + (\zeta_2' + \zeta_1\tau)\chi_2 - \zeta^2\mathrm{T}].$$

Substituting into the definitions of ζ_{χ_2} and τ_{χ_2} yields the desired results. □

Remark 4.3. *Setting $\tau = 0$ in* (4.8) *and* (4.9) *produces the formulas for the second Bishop spherical indicatrix.*

4.4. Analytical linkage between $\mathbb{B}$-Darboux helices and their spherical curves

Theorem 4.4. *If $\varphi(\sigma)$ is a Type-I generalized $\mathbb{B}$-helix, then its tangent spherical image ψ_{T} is a circle on $\mathbb{S}^2$.*

Proof. For a Type-I generalized $\mathbb{B}$-helix, the ratio ζ_1/ζ_2 is constant. Consequently, $\zeta_1'\zeta_2 - \zeta_2'\zeta_1 = 0$, and Eq (4.2) implies $\zeta_{\mathrm{T}} =$ constant. Hence, ψ_{T} is a circle. □

Theorem 4.5. *If $\varphi(\sigma)$ is a Type-II (resp. Type-III) generalized $\mathbb{B}$-helix, then the corresponding spherical image ψ_{χ_1} (resp. ψ_{χ_2}) is a circle on $\mathbb{S}^2$.*

Proof. For a Type-II generalized $\mathbb{B}$-helix, the condition

$$\frac{d}{d\sigma}\left(\frac{\zeta_2}{\zeta}\right) + \tau\left(\frac{\zeta_1}{\zeta}\right) = 0$$

implies proportional variation of ζ_1 and ζ_2, leading to ζ_{χ_1} = constant from (4.5). An analogous argument, using (4.8), shows that ψ_{χ_2} is circular for a Type-III helix. □

Remark 4.4. *Each class of generalized $\mathbb{B}$-helices corresponds to a circular image on the unit sphere: the tangent circle (Type-I), χ_1-circle (Type-II), and χ_2-circle (Type-III). This correspondence extends the geometric relationship known for the Bishop and Darboux frameworks to the $\mathbb{B}$-Darboux setting.*

5. Representative examples and geometric visualizations

In this section, several explicit examples are presented to illustrate the geometric behavior of generalized $\mathbb{B}$-helices and their spherical counterparts within the framework of the $\mathbb{B}$-Darboux frame. The purpose is to validate the theoretical results derived earlier through concrete constructions and numerical visualizations. For each example, we consider a smooth unit-speed curve constrained to a surface and compute the associated Frenet, Darboux, and $\mathbb{B}$-Darboux frame vectors together with their curvature invariants. Based on these data, the corresponding $\mathbb{B}$-Darboux helices and the ruled surfaces generated by the directions χ_1 and χ_2 are constructed, including cases with torsion degeneracy. The Gaussian and mean curvatures of the resulting surfaces are then evaluated to analyze their intrinsic and extrinsic geometric properties, while the accompanying plots provide visual insight into the role of the $\mathbb{B}$-Darboux curvatures in shaping the curves and induced ruled surfaces in E^3.

Example 5.1. *Consider the regular unit-speed helix*

$$\varphi(\sigma) = \frac{1}{\sqrt{2}}(\cos\sigma, \sin\sigma, \sigma), \qquad \sigma \in \mathbb{R}.$$

Its Frenet apparatus may be calculated as follows:

$$\begin{aligned}
\mathrm{T}(\sigma) &= \frac{1}{\sqrt{2}}(-\sin\sigma, \cos\sigma, 1),\\
\mathrm{N}(\sigma) &= (-\cos\sigma, -\sin\sigma, 0),\\
\mathrm{B}(\sigma) &= \frac{1}{\sqrt{2}}(\sin\sigma, -\cos\sigma, 1),\\
\zeta(\sigma) &= \frac{1}{\sqrt{2}}, \quad \tau(\sigma) = \frac{1}{\sqrt{2}}.
\end{aligned}$$

Assume that φ lies on the right cylindrical surface

$$\mathbb{M}: \ x^2 + y^2 = \tfrac{1}{2},$$

whose unit normal is

$$n(\sigma) = (\cos\sigma, \sin\sigma, 0).$$

The Darboux frame $\{\mathrm{T}, g, n\}$ *is then given by*

$$g(\sigma) = (-\sin\sigma, \cos\sigma, 0), \qquad n(\sigma) = (\cos\sigma, \sin\sigma, 0),$$
$$\zeta_g = 0, \qquad \zeta_n = -\frac{1}{\sqrt{2}}, \qquad \tau_g = -1.$$

For the helix, $\zeta = \tau = \frac{1}{\sqrt{2}}$*, and choosing* $\theta(\sigma) = \sigma/\sqrt{2}$*, the* $\mathbb{B}$*–Darboux frame and its curvatures are given by (see Figure 1).*

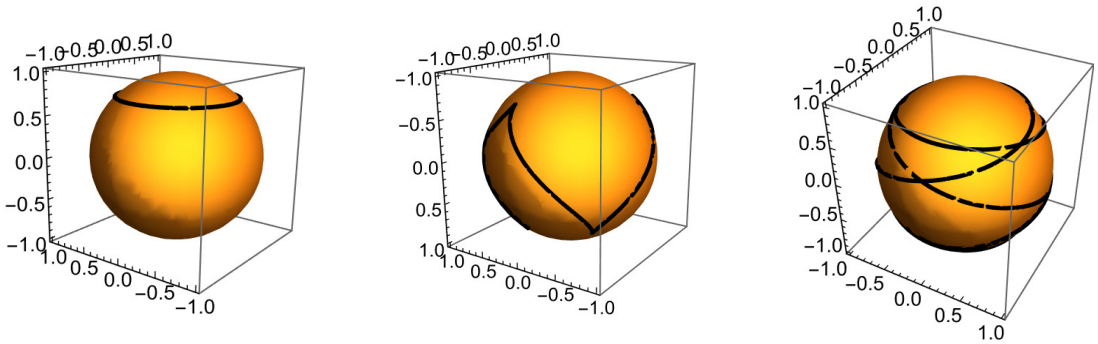

Figure 1. Spherical images $\psi_T(\sigma_{\mathrm{T}})$, $\psi_{\chi_1}(\sigma_{\chi_1})$, and $\psi_{\chi_2}(\sigma_{\chi_2})$ of $\varphi(\sigma)$.

$$\mathrm{T}(\sigma) = \frac{1}{\sqrt{2}}(-\sin\sigma, \cos\sigma, 1),$$
$$\chi_1(\sigma) = \begin{pmatrix} \cos\sigma\sin\left(\frac{\sigma}{\sqrt{2}}\right) + \frac{1}{\sqrt{2}}\sin\sigma\cos\left(\frac{\sigma}{\sqrt{2}}\right) \\ \sin\sigma\sin\left(\frac{\sigma}{\sqrt{2}}\right) - \frac{1}{\sqrt{2}}\cos\sigma\cos\left(\frac{\sigma}{\sqrt{2}}\right) \\ \frac{1}{\sqrt{2}}\cos\left(\frac{\sigma}{\sqrt{2}}\right) \end{pmatrix},$$
$$\chi_2(\sigma) = \begin{pmatrix} -\cos\sigma\cos\left(\frac{\sigma}{\sqrt{2}}\right) - \frac{1}{\sqrt{2}}\sin\sigma\sin\left(\frac{\sigma}{\sqrt{2}}\right) \\ -\sin\sigma\cos\left(\frac{\sigma}{\sqrt{2}}\right) + \frac{1}{\sqrt{2}}\cos\sigma\sin\left(\frac{\sigma}{\sqrt{2}}\right) \\ \frac{1}{\sqrt{2}}\cos\left(\frac{\sigma}{\sqrt{2}}\right) \end{pmatrix},$$
$$\zeta_1(\sigma) = \frac{1}{\sqrt{2}}\cos\left(\frac{\sigma}{\sqrt{2}}\right), \qquad \zeta_2(\sigma) = \frac{1}{\sqrt{2}}\sin\left(\frac{\sigma}{\sqrt{2}}\right).$$

Now, we define the developable ruled surface generated by χ_1 *as follows:*

$$\Phi(\sigma, \upsilon) = \varphi(\sigma) + \upsilon\chi_1(\sigma), \qquad (\sigma, \upsilon) \in I \times \mathbb{R}.$$

Define the unit normal as $n_{\chi_1} = \chi_1$, and the Gaussian and mean curvatures are computed as (see Figure 2)

$$K_\Phi(\sigma, \upsilon) = 0, \qquad H_\Phi(\sigma, \upsilon) = \frac{\sin\sigma}{4\left(1 - \frac{\upsilon}{2}\cos\sigma\right)}.$$

For $\upsilon = 0$, $H_\Phi(\sigma, 0) = \frac{1}{4}\sin\sigma$, so the surface alternately bends outward and inward along the helix.

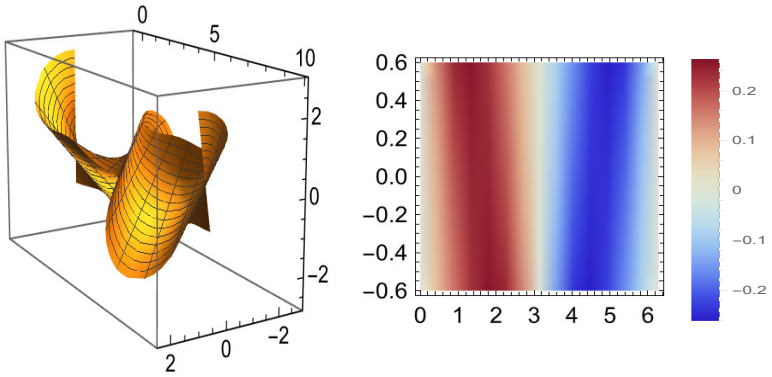

Figure 2. Developable ruled surface Φ generated by χ_1 and $H_\Phi(\sigma, \upsilon)$.

Analogously, we consider developable ruled surface generated by χ_2.

$$\Psi(\sigma, \upsilon) = \varphi(\sigma) + \upsilon\chi_2(\sigma).$$

We take the unit normal as $n_{\chi_2} = \chi_2$, so the Gaussian and mean curvatures are computed as (see Figure 3)

$$K_\Psi(\sigma, \upsilon) = 0, \qquad H_\Psi(\sigma, \upsilon) = -\frac{\cos\sigma}{4\left(1 - \frac{\upsilon}{2}\sin\sigma\right)}.$$

At $\upsilon = 0$, $H_\Psi(\sigma, 0) = -\frac{1}{4}\cos\sigma$, which oscillates with opposite phase to H_Φ.

The corresponding surface plots were generated numerically to visualize the geometric effect of the $\mathbb{B}$-Darboux directions and to confirm the analytical results.

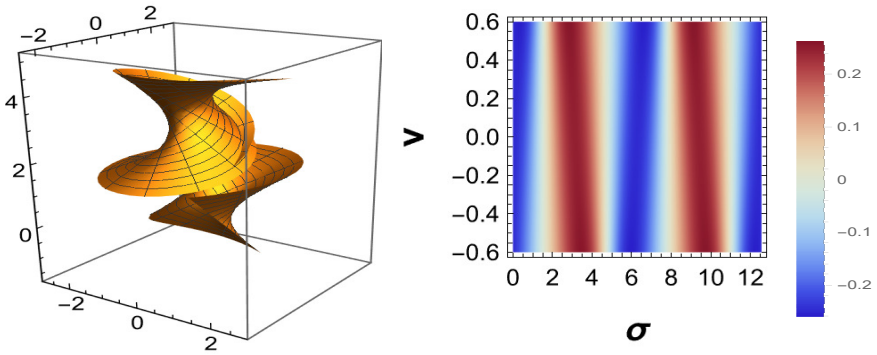

Figure 3. Developable ruled surface Ψ generated by χ_2 and $H_\Psi(\sigma, \upsilon)$.

Example 5.2. *Consider the regular unit speed ω defined by*

$$\omega(\sigma) = \left(12\cos\left(\frac{\sigma}{13}\right),\ 12\sin\left(\frac{\sigma}{13}\right),\ \frac{5\sigma}{13}\right), \qquad \sigma \in \mathbb{R}.$$

This curve lies entirely on the unit sphere $\mathbb{S}^2$ and is of unit-speed. The Frenet-Serret apparatus can be computed as the following:

$$\mathrm{T}(\sigma) = \Big(-\tfrac{12}{13}\sin\Big(\frac{\sigma}{13}\Big),\ \tfrac{12}{13}\cos\Big(\frac{\sigma}{13}\Big),\ \tfrac{5}{13}\Big),$$

$$\mathrm{N}(\sigma) = \Big(-\cos\Big(\frac{\sigma}{13}\Big),\ -\sin\Big(\frac{\sigma}{13}\Big),\ 0\Big),$$

$$\mathrm{B}(\sigma) = \Big(\tfrac{5}{13}\sin\Big(\frac{\sigma}{13}\Big),\ -\tfrac{5}{13}\cos\Big(\frac{\sigma}{13}\Big),\ \tfrac{12}{13}\Big),$$

$$\kappa(\sigma) = \tfrac{12}{169}, \quad \tau(\sigma) = \tfrac{5}{169}.$$

The $\mathbb{B}$-Darboux frame apparatus is given by (see Figure 4)

$$\mathrm{T}(\sigma) = \Big(-\tfrac{12}{13}\sin\Big(\frac{\sigma}{13}\Big),\ \tfrac{12}{13}\cos\Big(\frac{\sigma}{13}\Big),\ \tfrac{5}{13}\Big),$$

$$\chi_1(\sigma) = \Big(\tfrac{5}{13}\sin\Big(\tfrac{\sigma}{13}\Big)\sin\Big(\tfrac{5\sigma}{169}\Big) + \cos\Big(\tfrac{\sigma}{13}\Big)\cos\Big(\tfrac{5\sigma}{169}\Big), -\tfrac{5}{13}\cos\Big(\tfrac{\sigma}{13}\Big)\sin\Big(\tfrac{5\sigma}{169}\Big) + \sin\Big(\tfrac{\sigma}{13}\Big)\cos\Big(\tfrac{5\sigma}{169}\Big), \tfrac{12}{13}\sin\Big(\tfrac{5\sigma}{169}\Big)\Big),$$

$$\chi_2(\sigma) = \Big(-\tfrac{5}{13}\sin\Big(\tfrac{\sigma}{13}\Big)\cos\Big(\tfrac{5\sigma}{169}\Big) + \cos\Big(\tfrac{\sigma}{13}\Big)\sin\Big(\tfrac{5\sigma}{169}\Big), \tfrac{5}{13}\cos\Big(\tfrac{\sigma}{13}\Big)\cos\Big(\tfrac{5\sigma}{169}\Big) + \sin\Big(\tfrac{\sigma}{13}\Big)\sin\Big(\tfrac{5\sigma}{169}\Big), -\tfrac{12}{13}\cos\Big(\tfrac{5\sigma}{169}\Big)\Big),$$

$$\zeta_1(\sigma) = -\tfrac{12}{169}\sin\Big(\tfrac{5\sigma}{169}\Big), \qquad \zeta_2(\sigma) = \tfrac{12}{169}\cos\Big(\tfrac{5\sigma}{169}\Big).$$

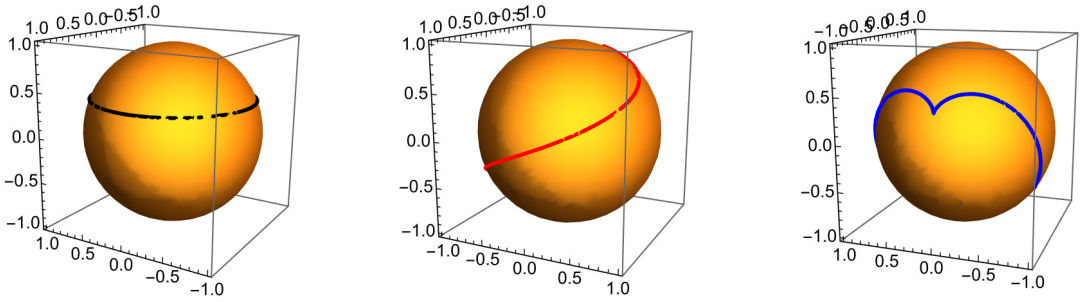

Figure 4. Spherical images $\psi_T(\sigma_{\mathrm{T}})$, $\psi_{\chi_1}(\sigma_{\chi_1})$, and $\psi_{\chi_2}(\sigma_{\chi_2})$ of $\omega(\sigma)$.

We construct the non-developable ruled surface generated by χ_1 as follows (see Figure 5):

$$\Gamma(\sigma, \upsilon) = \omega(\sigma) + \upsilon\chi_1(\sigma), \qquad (\sigma, \upsilon) \in I \times \mathbb{R}.$$

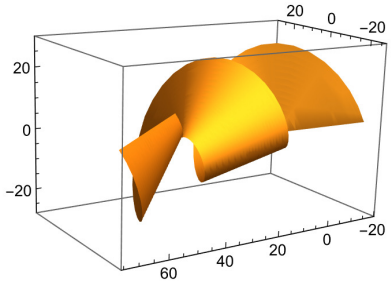

Figure 5. Non-developable ruled surface $\Gamma(\sigma, \upsilon)$.

From the $\mathbb{B}$-Darboux relations, we obtain

$$\Gamma(\sigma,\upsilon)=\omega(\sigma)+\upsilon\chi_1(\sigma),\qquad(\sigma,\upsilon)\in I\times\mathbb{R}.$$

From the $\mathbb{B}$-Darboux relations, we obtain (see Figures 6 and 7)

$$K_\Gamma(\sigma,\upsilon)=-\frac{\left[\frac{12}{169}\cos\left(\frac{5\sigma}{169}\right)\right]^2}{\left[1-\frac{12\upsilon}{169}\sin\left(\frac{5\sigma}{169}\right)\right]^2},$$
$$H_\Gamma(\sigma,\upsilon)=-\frac{\frac{12}{169}\sin\left(\frac{5\sigma}{169}\right)}{2\left[1-\frac{12\upsilon}{169}\sin\left(\frac{5\sigma}{169}\right)\right]^2}.$$

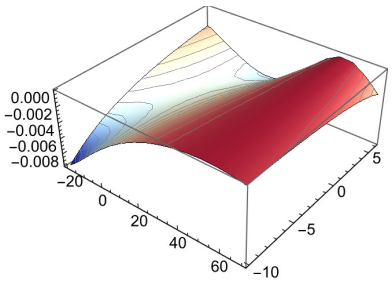

Figure 6. Gaussian curvature $K_\Gamma(\sigma,\upsilon)$.

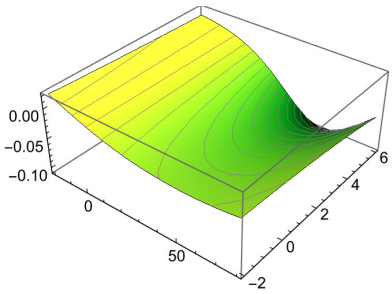

Figure 7. Mean curvature $H_\Gamma(\sigma,\upsilon)$.

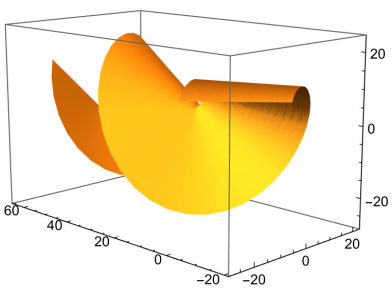

Figure 8. Non-developable ruled surface $\Omega(\sigma,\upsilon)$.

In addition to the surface generated by χ_1, we now define the non-developable ruled surface generated by χ_2 as follows (see Figure 8):

$$\Omega(\sigma, \upsilon) = \omega(\sigma) + \upsilon\chi_2(\sigma).$$

Thus, the Gaussian and mean curvatures of Ω are given by (see Figures 9 and 10)

$$K_\Omega(\sigma,\upsilon) = -\frac{\left[\frac{12}{169}\sin\left(\frac{5\sigma}{169}\right)\right]^2}{\left[1+\frac{12\upsilon}{169}\cos\left(\frac{5\sigma}{169}\right)\right]^2+\left[\frac{12\upsilon}{169}\sin\left(\frac{5\sigma}{169}\right)\right]^2},$$

$$H_\Omega(\sigma,\upsilon) = \frac{\frac{12}{169}\cos\left(\frac{5\sigma}{169}\right)}{2\left[\left(1+\frac{12\upsilon}{169}\cos\left(\frac{5\sigma}{169}\right)\right)^2+\left(\frac{12\upsilon}{169}\sin\left(\frac{5\sigma}{169}\right)\right)^2\right]}.$$

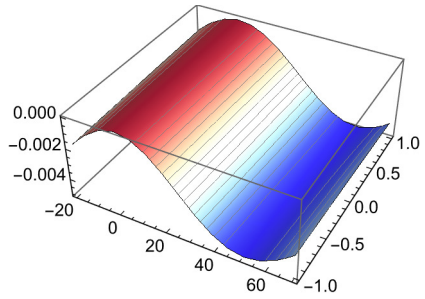

Figure 9. Gaussian curvature $K_\Omega(\sigma, \upsilon)$.

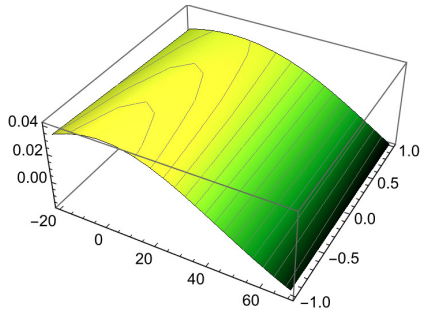

Figure 10. Mean curvature $H_\Omega(\sigma, \upsilon)$.

Example 5.3. *This example highlights a key advantage of the $\mathbb{B}$-Darboux framework: It offers a surface-adapted, torsion regular description that unifies intrinsic and extrinsic curvature information even in regimes where traditional frame=based approaches lose effectiveness.*

Consider the smooth unit-speed curve $\phi : \mathbb{R} \to \mathrm{E}^3$ defined by

$$\phi(\sigma) = (\cos\sigma,\ \sin\sigma,\ \varepsilon\sin\sigma), \qquad 0 < \varepsilon \leq 1,$$

which lies on the smooth cylindrical surface $\mathbb{M} : x^2 + y^2 = 1$. *The Frenet apparatus of* ϕ *is given by*

$$\kappa(\sigma) = \frac{\sqrt{1 + \varepsilon^2 \cos^2 \sigma}}{(1 + \varepsilon^2)^{3/2}},$$
$$\tau(\sigma) = \frac{\varepsilon \sin \sigma}{1 + \varepsilon^2 \cos^2 \sigma}.$$

In particular, the torsion $\tau(\sigma)$ *vanishes at* $\sigma = k\pi$, $k \in \mathbb{Z}$, *causing instability in Frenet-based descriptions. The Bishop frame remains well defined; however, it does not encode the surface geometry of* $\mathbb{M}$ *and fails to distinguish intrinsic and extrinsic curvature effects induced by the constraint* $x^2 + y^2 = 1$.

Let $n(\sigma) = (\cos \sigma, \sin \sigma, 0)$ *denote the unit normal of the cylinder M, and let* $g = n \times \mathrm{T}$. *The Darboux curvatures are*

$$\kappa_g(\sigma) = 0, \qquad \kappa_n(\sigma) = -\frac{1}{\sqrt{1 + \varepsilon^2}}.$$

Define the $\mathbb{B}$*-Darboux rotation angle by*

$$\vartheta(\sigma) = \int_0^\sigma \tau(s)\, ds = \arctan(\varepsilon \tan \sigma),$$

which is continuous even at points where $\tau(\sigma) = 0$. *The corresponding* $\mathbb{B}$*-Darboux frame and the curvatures are*

$$\mathrm{T}(\sigma) = \frac{1}{\sqrt{1 + \varepsilon^2 \cos^2 \sigma}}(-\sin \sigma,\ \cos \sigma,\ \varepsilon \cos \sigma),$$
$$\chi_1(\sigma) = \sin \vartheta(\sigma)\, g(\sigma) + \cos \vartheta(\sigma)\, n(\sigma),$$
$$\chi_2(\sigma) = -\cos \vartheta(\sigma)\, g(\sigma) + \sin \vartheta(\sigma)\, n(\sigma),$$
$$\zeta_1(\sigma) = \kappa_g \cos \vartheta + \kappa_n \sin \vartheta = -\frac{\sin \vartheta(\sigma)}{\sqrt{1 + \varepsilon^2}},$$
$$\zeta_2(\sigma) = \kappa_g \sin \vartheta - \kappa_n \cos \vartheta = \frac{\cos \vartheta(\sigma)}{\sqrt{1 + \varepsilon^2}}.$$

Both ζ_1 *and* ζ_2 *are smooth and non-singular for all* σ. *This confirms that the* $\mathbb{B}$*-Darboux frame provides a stable and surface-adapted description of the curve geometry even in the presence of torsion degeneracy. Using the* $\mathbb{B}$*-Darboux frame vectors* χ_1 *and* χ_2, *we define the ruled surfaces (see Figures 11 and 12).*

$$\Lambda(\sigma, v) = \phi(\sigma) + v\, \chi_1(\sigma),$$
$$\Theta(\sigma, v) = \phi(\sigma) + v\, \chi_2(\sigma),$$

where $(\sigma, v) \in I \times \mathbb{R}$. *Hence, the Gaussian and mean curvatures of* Λ *are (see Figure 13)*

$$K_\Lambda = 0, \quad H_\Lambda = \frac{(1 - v\zeta_1)\zeta_2}{2(1 - v\zeta_1)^2} = \frac{\zeta_2}{2(1 - v\zeta_1)}.$$

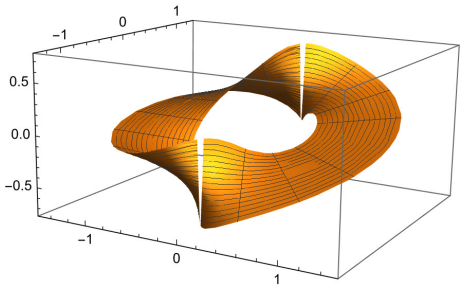

Figure 11. Developable ruled surface $\Lambda(\sigma, \upsilon)$.

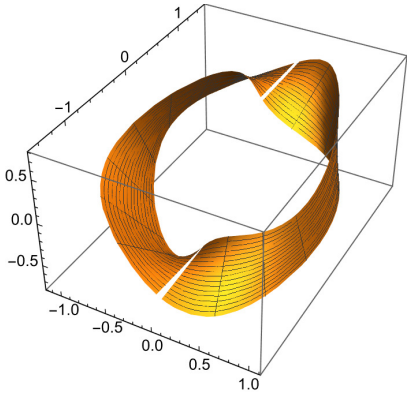

Figure 12. Developable ruled surface $\Theta(\sigma, \upsilon)$.

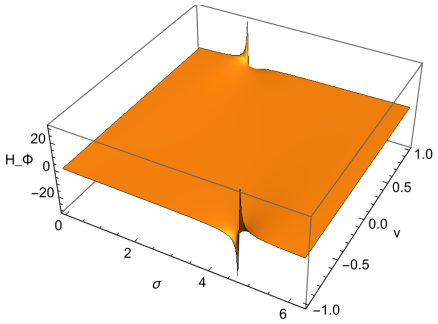

Figure 13. Mean curvature $H_\Lambda(\sigma, \upsilon)$..

Therefore, Λ is a developable ruled surface with nonzero mean curvature, whose bending behavior is governed by the $\mathbb{B}$-Darboux curvatures. Also, the Gaussian and mean curvatures of Θ are (see Figure 14)

$$K_\Theta = 0, \quad H_\Theta = \frac{(1 - v\zeta_2)\zeta_1}{2(1 - v\zeta_2)^2} = \frac{\zeta_1}{2(1 - v\zeta_2)}.$$

Both ruled surfaces Φ and Θ are developable; however, their mean curvature distributions differ substantially, reflecting the asymmetric roles of the $\mathbb{B}$-Darboux curvatures ζ_1 and ζ_2.

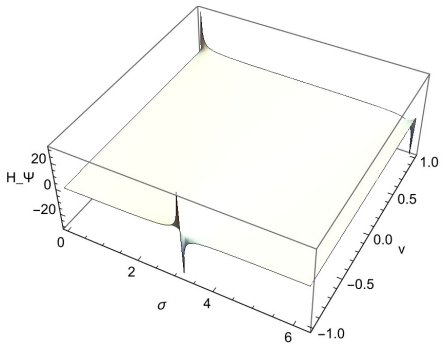

Figure 14. Mean curvature $H_\Theta(\sigma, \upsilon)$.

6. Concluding observations and future directions

Rather than introducing an alternative moving frame in isolation, the present work proposes a unifying curvature formulation for surface constrained curves in $\mathbb{E}^3$. Through a torsion-driven rotation of the classical Darboux frame, the intrinsic and extrinsic curvature effects are encoded into a coupled pair of invariants, allowing several known helical structures to be recovered within a single geometric framework.

In this sense, the $\mathbb{B}$-Darboux formulation should be viewed as a structural extension of Frenet, Bishop, and Darboux descriptions, rather than a competing construction. Its strength lies in its ability to provide a stable, surface-adapted curvature model that remains effective in degenerate or transitional regimes, and naturally supports the generation and analysis of ruled surfaces associated with surface-bound curves.

For each class, precise necessary and sufficient conditions are established via differential relations involving the invariants (ζ_1, ζ_2). In addition, the induced spherical curves corresponding to the vectors T, χ_1, and χ_2 are examined in detail, and explicit expressions for their curvature and torsion are derived. A notable outcome is that every generalized $\mathbb{B}$-helix admits a circular spherical image, thereby revealing a direct correspondence between the spatial geometry of the curve and its representation on the unit sphere. Several examples, including curves traced on cylindrical and spherical surfaces, illustrate the applicability of the framework and its effectiveness in the construction and analysis of non-developable ruled surfaces.

The proposed formulation extends and unifies earlier descriptions based on Frenet, Bishop, and flow frames by offering a surface-adapted representation that remains well defined even in degenerate situations such as vanishing torsion. In this sense, the $\mathbb{B}$-Darboux frame provides a stable geometric tool for capturing both kinematic and curvature-related features of surface-bound curves. Its continuity and adaptability make it particularly suitable for theoretical investigations as well as computational treatments of geometric evolution and deformation processes.

Although the present work is formulated for curves lying on smooth surfaces in E^3, the underlying ideas admit several natural extensions. Variants independent of a supporting surface may be developed by reinterpreting the rotation in terms of Frenet or Bishop frames, while generalizations to Riemannian manifolds or Lie groups can be pursued using appropriate orthonormal frames and connection structures. From a numerical perspective, the non-local rotation angle $\vartheta(s)$ can be

approximated through discretization or spline-based techniques, enabling practical implementations in geometric design and motion planning. Furthermore, embedding the invariants (ζ_1, ζ_2) into variational or energy-based formulations offers a promising direction for linking the $\mathbb{B}$-Darboux framework with models arising in elasticity, mechanics, and curvature-driven optimization.

Author contributions

All authors contributed equally. All authors have read and agreed to the published version of the manuscript.

Use of Generative-AI tools declaration

The authors declare they have not used Artificial Intelligence (AI) tools in the creation of this article.

Acknowledgements

This work was supported and funded by the Deanship of Scientific Research at Imam Mohammad Ibn Saud Islamic University (IMSIU) (grant number IMSIU-DDRSP2601).

Conflicts of interest

The authors declare no conflicts of interest in this paper.

References

1. A. T. Ali, R. López, Slant helices in Minkowski space E_1^3, *J. Korean Math. Soc.*, **48** (2011), 159–167. https://doi.org/10.4134/JKMS.2011.48.1.159
2. M. T. Aldossary, R. A. Abdel-Baky, Sweeping surface due to rotation minimizing Darboux frame in Euclidean 3-space E_1^3, *AIMS Mathematics*, **8** (2023), 447–462. https://doi.org/10.3934/math.2023021
3. I. Al-Dayel, E. Solouma, M. Khan, On geometry of focal surfaces due to B-Darboux and type-2 Bishop frames in Euclidean 3-space, *AIMS Mathematics*, **7** (2022), 13454–13468. https://doi.org/10.3934/math.2022744
4. M. Barros, General helices and a theorem of Lancret, *P. Am. Math. Soc.*, **125** (1997), 1503–1509.
5. M. Barros, A. Ferrández, P. Lucas, M. A. Meroaño, General helices in the three-dimensional Lorentzian space forms, *Rocky Mountain J. Math.*, **31** (2001), 373–388. https://doi.org/10.1216/rmjm/1020171565
6. B. Bükcü, M. K. Karacan, On the modified orthogonal frame with curvature and torsion in Minkowski 3-space, *Math. Sci. Appl. E-Notes*, **4** (2016), 184–188. https://doi.org/10.36753/mathenot.421429
7. B. Bükcü, M. K. Karacan, Spherical curves with modified orthogonal frame, *J. New Results Sci.*, **6** (2016), 60–68.

8. A. Cayley, Mémoire sur les courbes à double courbure et les surfaces développables, *Journal de mathématiques pures et appliquées 1re série*, **10** (1845), 245–250.
9. Ü. Çiftçi, A generalization of Lancret's theorem, *J. Geom. Phys.*, **59** (2009), 1597–1603. https://doi.org/10.1016/j.geomphys.2009.07.016
10. M. Crasmareanu, The flow-curvature of spacelike parametrized curves in the Lorentz plane, *Proc. Int. Geom. Cent.*, **15** (2022), 101–109. https://doi.org/10.15673/tmgc.v15i2.2281
11. M. Crasmareanu, The flow-curvature of plane parametrized curves, *Commun. Fac. Sci. Univ.*, **72** (2023), 417–428.
12. M. Crasmareanu, The flow-geodesic curvature and the flow-evolute of hyperbolic plane curves, *Int. Electron. J. Geom.*, **16** (2023), 1–6.
13. M. Crasmareanu, The flow-curvature of curves on geometric surfaces, *Commun. Korean Math. Soc.*, **38** (2023), 1261–1269. https://doi.org/10.4134/CKMS.c230024
14. M. Dede, M. Ç. Aslan, C. Ekici, On a variational problem due to the B-Darboux frame in Euclidean 3-space, *Math. Methods Appl. Sci.*, **44** (2021), 12630–12639. https://doi.org/10.1002/mma.7567
15. M. P. do Carmo, *Differential geometry of curves and surfaces*, New York: Dover Publications, 2016.
16. H. K. Elsayied, A. A. Altaha, A. Elsharkawy, On some special curves according to the modified orthogonal frame in Minkowski 3-space E_1^3, *KASMERA*, **49** (2021), 2–15.
17. K. Eren, H. H. Koşal, Evolution of space curves and the special ruled surfaces with modified orthogonal frame, *AIMS Mathematics*, **5** (2020), 2027–2039. https://doi.org/10.3934/math.2020134
18. A. Ferrández, A. Giménez, P. Lucas, Null generalized helices in Lorentz–Minkowski spaces, *J. Phys. A: Math. Gen.*, **35** (2002), 8243. https://doi.org/10.1088/0305-4470/35/39/308
19. S. Izumiya, N. Takeuchi, New special curves and developable surfaces, *Turk. J. Math.*, **28** (2004), 153–164.
20. L. Kula, Y. Yaylı, On slant helix and its spherical indicatrix, *Appl. Math. Comput.*, **169** (2005), 600–607. https://doi.org/10.1016/j.amc.2004.09.078
21. L. Kula, N. Ekmekci, Y. Yaylı, K. İlarslan, Characterizations of slant helices in Euclidean 3-space, *Turk. J. Math.*, **34** (2010), 261–274. https://doi.org/10.3906/mat-0809-17
22. M. A. Lancret, Mémoire sur les courbes à double courbure, *Memoires presentes alInstitut*, **1** (1806), 416–454.
23. P. Lucas, J. A. Ortega-Yagües, Slant helices in the Euclidean 3-space revisited, *Bull. Belg. Math. Soc. Simon Stevin*, **23** (2016), 133–150.
24. P. Lucas, J. A. Ortega-Yagües, Slant helices in the three-dimensional sphere, *J. Korean Math. Soc.*, **54** (2017), 1331–1343. https://doi.org/10.4134/JKMS.j160508
25. P. Lucas, J. A. Ortega-Yagües, Slant helices: A new approximation, *Turk. J. Math.*, **43** (2019), 473–485. https://doi.org/10.3906/mat-1809-16

26. B. Li, L. Zhu, Turing instability analysis of a reaction–diffusion system for rumor propagation in continuous space and complex networks, *Inf. Process. Manag.*, **61** (2024), 103621. https://doi.org/10.1016/j.ipm.2023.103621

27. O. Z. Okuyucu, I. Gök, Y. Yayli, N. Ekmekci, Slant helices in three-dimensional Lie groups, *Appl. Math. Comput.*, **221** (2013), 672–683. https://doi.org/10.1016/j.amc.2013.07.008

28. U. Öztürk, Z. B. Alkan, Darboux helices in three-dimensional Lie groups, *AIMS Mathematics*, **5** (2020), 3169–3181. https://doi.org/10.3934/math.2020204

29. C. Ö. Anar, Y. Yayli, N. Ekmekci, Generalized helices in Euclidean 3-space through the flow frame, *Int. Electron. J. Geom.*, **18** (2025), 335–348. https://doi.org/10.36890/iejg.1691504

30. E. M. Solouma, I. Al-Dayel, Harmonic evolute surface of tubular surfaces via the *B*-Darboux frame, *Adv. Math. Phys.*, 2021. https://doi.org/10.1155/2021/5269655

31. E. Solouma, I. Al-Dayel, M. A. Abdelkawy, Ruled surfaces and their geometric invariants via the orthogonal modified frame in Minkowski 3-space, *Mathematics*, **13** (2025), 940. https://doi.org/10.3390/math13060940

32. D. J. Struik, *Lectures on classical differential geometry*, New York: Dover Publications, 1988.

33. H. Sha, L. Zhu, Dynamic analysis of pattern and optimal control research of rumor propagation model on different networks, *Inform. Process. Manag.*, **62** (2025), 104016. https://doi.org10.1016/j.ipm.2024.104016

AIMS Press